

# Relative Thermodynamic Stability of DNA, RNA, and DNA:RNA Hybrid Duplexes: Relationship with Base Composition and Structure

Elena A. Lesnik\* and Susan M. Freier

Department of Structural Biology, ISIS Pharmaceuticals, 2292 Faraday Avenue, Carlsbad, California 92008

Received February 28, 1995; Revised Manuscript Received June 14, 1995<sup>®</sup>

**ABSTRACT:** Fourteen oligonucleotides 8–21 nucleotides in length and their complements were synthesized as DNA and RNA. For each sequence, four kinds of duplexes, DNA:DNA, RNA:RNA, DNA:RNA, and RNA:DNA, were prepared. Twelve sequences had A•T/U content varying from 25 to 80% and dPy content in the DNA strands varying from 0 to 100%. Thermodynamic stabilities of four duplexes for each sequence were determined in solution containing 100 mM Na<sup>+</sup>, 10 mM phosphate, and 0.1 mM EDTA, pH 7.1. CD spectra and electrophoretic mobility on native polyacrylamide gel were measured for most duplexes. Quantitative correlations of hybrid stability both with deoxypyrimidine content and, at fixed dPy content, with the fraction of A•T/U in duplexes were found. We also demonstrated that hybrids with 70–80% deoxypyrimidine DNA strand and a high or moderate A•T/U fraction displayed the highest relative stability compared to their RNA counterparts. Relationships of relative intensities of CD bands at 210 nm and relative electrophoretic mobilities of hybrids with relative hybrid stability suggested that hybrid conformation varies continuously between A- and B-form and is the decisive factor in relative hybrid stability.

RNA:DNA complementary hybridization is an important part of many processes occurring in cells. Hybrids form during straight and reverse transcription (Varmus, 1982), initiation of DNA replication (Ogawa & Okazaki, 1980), and recombination (Kirkpatrick & Radding, 1992). Special interest in the structure and stability of heteroduplexes has arisen recently with development of antisense oligonucleotides as novel antiviral and anticancer therapeutics (Crooke, 1992). Elucidation of a relationship between sequence, conformation, and stability of hybrids is important for extension of our fundamental concepts as well as for the development of antisense drug technology.

On the basis of the first CD<sup>1</sup> (Gray & Ratliff, 1975), NMR (Pardi et al., 1981), and X-ray filament diffraction (O'Brien & MacEvan, 1970) data, the conformation of heteroduplexes in solution or under highly hydrated conditions was thought to be more similar to that of double-stranded RNA than B-form DNA. Later, NMR and Raman spectroscopy studies (Shindo & Matsumoto, 1984; Fujiwara & Shindo, 1985; Benevides & Thomas, 1988) and X-ray diffraction studies (Arnott et al., 1986) led to the conclusion that the DNA and RNA strands of heteroduplexes have two distinct backbone conformations. PAGE and CD data on oligonucleotide duplexes also suggest that the conformation of DNA:RNA hybrids is intermediate between DNA and RNA geometry (Bhattacharyya et al., 1990; Roberts & Crothers, 1992; Ratmeyer et al., 1994; Hung et al., 1994). High-resolution two-dimensional NMR (Chou et al., 1989; Salazar et al., 1993; Fedoroff et al., 1993) and Raman experiments in solution (Katahira et al., 1990) confirmed that the sugar moieties of the RNA strand are in a 3'-endo conformation, while the conformation of DNA sugars belongs to the

B-family but differs from 2'-endo. Recent NMR studies and molecular dynamics simulations on a mixed purine–pyrimidine hybrid duplex carried out by Gonzales et al. (1994, 1995) suggest that in the DNA strand there is a two-state dynamic equilibrium between N- and S-type sugar conformers with the major conformer in the S domain.

Data reported to date primarily concern the stability of homopurine–homopyrimidine hybrid duplexes. Melting experiments indicated that the stability of homopurine–homopyrimidine polymer and oligomer duplexes decreases in the order (rPu)(rPy) > (rPu)(dPy) > (dPu)(dPy) > (dPu)(rPy) (Chamberlin & Patterson, 1965; Roberts & Crothers, 1992; Hung et al., 1994). The stability of polymer and oligomer duplexes with long (A)<sub>n</sub>(T/U)<sub>n</sub> stretches changes in another way: (dA)(dT) > (rA)(dT) > (rA)(rU) ≫ (dA)(rU) (Riley et al., 1966; Martin & Tinoco, 1980). Only two studies on random purine–pyrimidine sequences have been reported (Hall & McLaughlin, 1991; Ratmeyer et al., 1994). Results obtained in these experiments indicate that thermodynamic stability of duplexes decreases in order R:R > D:D > hybrids; i.e., the stability of hybrids is less than those of RNA and DNA duplexes.

Previous studies of hybrid stability were performed under nonphysiological conditions (Hall & McLaughlin, 1991; Roberts & Crothers, 1992; Ratmeyer et al., 1994) or used homopurine–homopyrimidine or repeated sequences (Roberts & Crothers, 1992; Ratmeyer et al., 1994; Hung et al., 1994). Most targets for antisense oligonucleotides have random purine–pyrimidine base composition. Therefore, it was important to find out whether relations between hybrid base composition and thermodynamic stability found for single special sequences are maintained for hybrids with a wide variety of pyrimidine and A•T/U content under conditions close to physiological. Fourteen oligonucleotides and their complements were synthesized as DNA and RNA. For each sequence, four kinds of duplexes, DNA:DNA (DD), RNA:RNA (RR), DNA:RNA (DR), and RNA:DNA (RD),

\*To whom correspondence should be addressed.

<sup>®</sup> Abstract published in *Advance ACS Abstracts*, August 15, 1995.

<sup>1</sup> Abbreviations: dPy, deoxypyrimidines; dPu, deoxypurines; CD, circular dichroism; NMR, nuclear magnetic resonance; PAGE, polyacrylamide gel electrophoresis; seq, sequence; bp, base pair(s).

were prepared and their thermodynamic stabilities were measured. We demonstrate below quantitative correlations of hybrid stability both with deoxypyrimidine content in DNA strand and, at fixed pyrimidine content, with the fraction of A·T/U in the duplex. CD spectra and native gel electrophoretic mobilities of hybrids measured for many sequences varied continuously between those observed for RR and DD duplexes and correlated with the relative stability of hybrid duplexes.

## MATERIALS AND METHODS

**Oligonucleotide Synthesis.** DNA and RNA oligonucleotides were synthesized using standard phosphoramidite procedures as described elsewhere (Monia et al., 1992). Oligonucleotides were analyzed by electrophoresis on 20% polyacrylamide denaturing gels and demonstrated to be at least 90% full-length.

**Determination of Hybridization Thermodynamics.** Absorbance vs temperature profiles were measured on a Gilford Response spectrophotometer at 4  $\mu$ M each strand in buffer containing 100 mM Na<sup>+</sup>, 10 mM phosphate, and 0.1 mM EDTA (pH 7.1). Oligonucleotide concentrations were determined as described previously (Lesnik et al., 1993).  $T_M$ s and free energies of duplex formation were obtained from fits of the data to a two-state model with linear sloping base lines (Petersheim & Turner, 1983). Each  $T_M$  or  $\Delta G^\circ_{37}$  and associated error bar represents the average value and standard deviation derived from at least three experiments. Error bars smaller than the symbol were omitted from the plots.

**Circular Dichroism Spectra.** CD spectra at 20 °C were recorded at 3  $\mu$ M each strand in melting buffer using a JASCO J-600 spectropolarimeter. Ellipticities of duplexes were converted to  $\Delta\epsilon$  and are reported per mole of residues. Relative intensities of the hybrid bands at 210 nm were calculated as the ratio  $\Delta\Delta\epsilon_{210}(\text{RR-hybrid})/\Delta\Delta\epsilon_{210}(\text{RR-DD})$ .

**Polyacrylamide Native Gel Electrophoresis of Oligonucleotide Duplexes.** The mobilities of oligonucleotide duplexes (RR, DR, RD, and DD) were examined on 20% polyacrylamide gels in buffer containing 40 mM Tris-boric acid and 1 mM MgCl<sub>2</sub>, pH 7.1 (TBM). The solutions of duplexes used for CD experiments were also used for PAGE experiments. Oligonucleotide duplexes in gel were visualized by StainsAll (Sigma) and analyzed by use of a Molecular Dynamics computing densitometer. Relative mobilities of RNA and DNA duplexes were calculated as the ratio of the distance between the start point and the oligonucleotide position to the distance between the start point and the position on the gel of the dye bromophenol blue and are the average of three or four experiments. Relative mobilities of hybrids were calculated as the ratio of the distance between RR and DR/RD duplexes to the distance between RR and DD duplexes. Data presented are the averaged values and standard deviations obtained from three independent experiments.

## RESULTS

**Thermodynamic Stability of RNA, DNA, and Hybrid Duplexes.** The base compositions of fourteen oligonucleotides from 8 to 21 nucleotides in length and their complements are listed in Table 1. Pyrimidine content in the DNA sequences varied from 0 to 100%, and A·T/U content varied from 25 to 80%. The sequences were divided into three

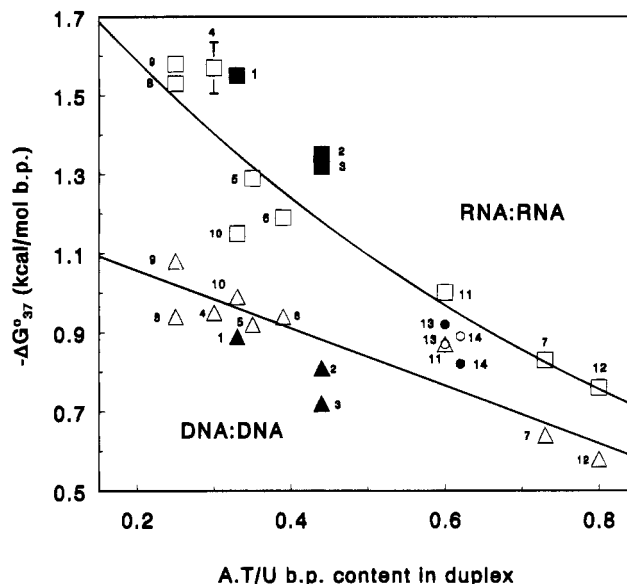


FIGURE 1: Effect of A·T/U content on free energy of RNA and DNA duplex formation: Free energies for RNAs of groups B and C (□), group A (■), and group D (●) and for DNAs of groups B and C (△), group A (▲), and group D (○). The solid lines are drawn through the data for duplexes of groups B and C. In this and subsequent figures, error bars are plotted only if they were greater than the size of the symbol ( $\pm 0.02$  kcal/mol of base pairs). Numbers near the markers designate numbers of the sequences in Table 1.

groups according to pyrimidine content in hybrid DNA strands (groups A–C). Group A contained three homopurine–homopyrimidine sequences (seqs 1–3). Group B contained four sequences (seqs 4–7) with high (70–78%) and low (22–30%) fractions of dPy in the hybrids. Group C contained five sequences (seqs 8–12) with 47–53% dPy in the hybrids. Two sequences contained (dA)<sub>n</sub> tracts which made up 33% (seq 13) or 62% (seq 14) of the sequence. These were assigned to group D because, as we will show, sequences with (A)<sub>n</sub> tracts provided exceptions to our generalizations.

Absorbance vs temperature curves were obtained for all sequences as four duplexes: RNA:RNA (RR), DNA:DNA (DD), DNA:RNA (DR), and RNA:DNA (RD). Temperatures of melting ( $T_M$ ) and  $\Delta G^\circ_{37}$  values are listed in Table 1. Although  $T_M$ s are not thermodynamic parameters, we included both  $T_M$  and  $\Delta G^\circ_{37}$  data because the  $T_M$  data were more precise than the  $\Delta G^\circ_{37}$  values. Correlations presented below were similar for both  $\Delta G^\circ_{37}$  and  $\Delta T_M$  values.

**Relative Stability of RNA and DNA Duplexes.** Figure 1 plots  $\Delta G^\circ_{37}$  vs fraction of A·T/U base pairs for DNA and RNA duplexes. The solid curves in this and subsequent figures were drawn to emphasize the trends observed. Figure 1 demonstrates that all the DNAs were less stable than the RNAs except seq 14. The decrease of (rA·rU) content resulted in the increase of the RNA duplex stability from 0.75 kcal/mol of base pairs for 80% (rA·rU) to 1.6 kcal/mol base pairs for 25% (rA·rU). Stability of the DNA duplexes increased linearly from 0.6 to 1 kcal/mol of base pairs under the same range of (dA·dT) content. For the homopurine–homopyrimidine duplexes (seqs 1–3 in Figure 1), the RNA duplexes were 0.2–0.25 kcal/mol of base pairs more stable and the DNA duplexes were 0.07–0.15 kcal/mol of base pairs less stable than predicted by the correlation observed for mixed purine–pyrimidine sequences (groups B and C).

Table 1: Free Energy and  $T_M$  Data for Oligonucleotide Duplexes

sequences	A•T/U <sup>a</sup> bp (%)	dPy <sup>b</sup> (%)	<i>T</i> <sub>M</sub> (°C)				−Δ <i>G</i> <sup>°</sup> <sub>37</sub> (kcal/mol of strands)				
			RR <sup>c</sup>	DD	DR	RD	RR	DD	DR	RD	
Group A											
(1) 5′-TCC CTC CTC TCC <sup>d</sup> 3′-AGG GAG GAG AGG	33	100 0	71.2	47.3	61.4	43.4	18.6	10.7	15.6	9.6	
(2) 5′-CCT TCC CTT 3′-GGA AGG GAA	44	100 0	52.9	32.6	44.8	20.5	12.2	7.3	10.0	5.8	
(3) 5′-TTC CCT TCC 3′-AAG GGA AGG	44	100 0	51.6	28.5	44.2	14.9	11.9	6.5	10.1	5.1	
Group B											
(4) 5′-GCT CTC TGG C 3′-CGA GAG ACC G	30	70 30	62.4	43.7	50.9	40.8	15.7	9.5	11.2	8.9	
(5) 5′-CTC GTA CCT TCC GGT CC 3′-GAG CAT GGA AGG CCAGG	35	76 24	74.5	60.6	64.8	56.0	21.9	15.7	17.0	12.7	
(6) 5′-CTC GTA CCT TTC CGG TCC 3′-GAG CAT GGA AAG GCC AGG	39	78 22	74.2	61.7	65.2	56.8	21.3	16.9	18.1	14.6	
(7) 5′-TAG TTA TCT CTA TCT 3′-ATC AAT AGA GAT AGA	73	73 27	52.7	42.1	45.4	34.9	12.4	9.6	10.5	7.5	
Group C											
(8) 5′-GCA CAG CC 3′-CGT GTC GG	25	50 50	53.4	32.1	37.2	35.6	12.3	7.5	8.1	7.9	
(9) 5′-GAG CTC CCA GGC 3′-CTC GAG GGT CCG	25	50 50	73.7	54.0	60.3	56.7	18.9	12.9	14.3	13.4	
(10) 5′-GCC GAG GTC CAT GTC GTA CGC 3′-CGG CTC CAG GTA CAG CAT GCG	33	52 48	80.2	69.5	68.2	68.1	24.1	20.8	17.2	18.0	
(11) 5′-TGT ACG TCA CAA CTA 3′-ACA TGC AGT GTT GAT	60	53 47	60.4	53.3	50.6	49.2	15.1	13.0	11.8	11.2	
(12) 5′-TAT ACA AGT TAT CTA 3′-ATA TGT TCA ATA GAT	80	53 47	48.4	39.7	35.2	35.9	11.3	8.7	7.7	7.8	
Group D											
(13) 5′-CGA CTA TGC AAA AAC 3′-GCT GAT ACG TTT TTG	60	40 60	54.2	50.4	39.0	47.3	13.8	13.1	8.7	11.3	
(14) 5′-CGC AAA AAA AAA ACG C 3′-GCG TTT TTT TTT TGC G	62	25 75	51.2	54.1	28.7	50.2	13.1	14.2	5.9	13.0	

<sup>a</sup> A·T/U bp denotes the fraction of A·T/U base pairs (% of total base pair amount) in duplex. <sup>b</sup> dPy denotes the fraction of deoxypyrimidines (% of total base amount) in upper and lower DNA strands. <sup>c</sup> RR denotes RNA:RNA duplex. DD denotes DNA:DNA duplex. DR denotes hybrid with upper strand as DNA and lower strand as RNA. RD denotes hybrid with upper strand as RNA and lower strand as DNA. <sup>d</sup> This is the same sequence used by Roberts and Crothers (1992).

**Relative Stability of Hybrid Duplexes of Groups A–C.** We examined 14 pairs of DR and RD hybrids for the same sequences.  $\Delta G^\circ_{37}$  values for each DR and RD pair were plotted against the fraction of A·T/U base pairs (Figure 2). Data indicate that the average stability of each DR/RD pair generally increased with the decrease of A·T/U base pairs, but the stability of DR and RD hybrids within a pair varied widely. The difference in DR and RD stability for each hybrid pair correlated well with the difference in pyrimidine content in hybrid DNA strands (Figure 3). (The plot for  $\Delta T_M$  vs  $\Delta dPy$  content is included in supporting information.)

**Stability of Hybrids Relative to Their RNA and DNA Counterparts (Groups A–C).** We compared the stability of each hybrid with the stability of its RNA and DNA counterparts.  $\Delta G^\circ_{37}(\text{hybrid})/\Delta G^\circ_{37}(\text{RR})$  ratios were plotted against deoxypyrimidine fraction in hybrid DNA strand (Figure 4a). The increase of deoxypyrimidine fraction in DNA strand resulted in an increase in relative hybrid stability. Between 0 and 60% deoxypyrimidine,  $\Delta G^\circ_{37}(\text{hybrid})$  values increased from  $47 \pm 5\%$  to  $73 \pm 5\%$  of the corresponding  $\Delta G^\circ_{37}(\text{RR})$  values, and  $\Delta T_m(\text{RR-hybrid})$  decreased from 33 to 13 °C. (The plot for  $\Delta T_m(\text{RR-hybrid})$  vs dPy content is included in supporting information.) Between 60 and 100% deoxypyrimidine content, only 10% in relative  $\Delta G^\circ_{37}$  value and 4 °C in  $\Delta T_m$  were added (numbers are taken from the curve).

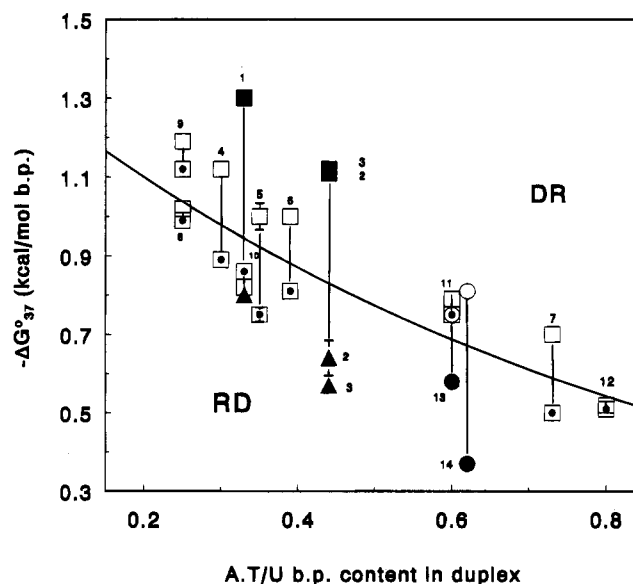


FIGURE 2: Effect of A·T/U content on free energy of DR and RD hybrid duplex formation: Free energies for DR hybrids of groups B and C (□), group A (■), and group D (●) and for RD hybrids of groups B and C (□), group A (▲), and group D (○). The solid line is drawn through the data for duplexes of group B and C.

Plotting  $\Delta G^\circ_{37}(\text{hybrid})/\Delta G^\circ_{37}(\text{DD})$  ratios against pyrimidine fraction in hybrid DNA strand (Figure 4b) demonstrates that relative hybrid stability compared to the DNA stability

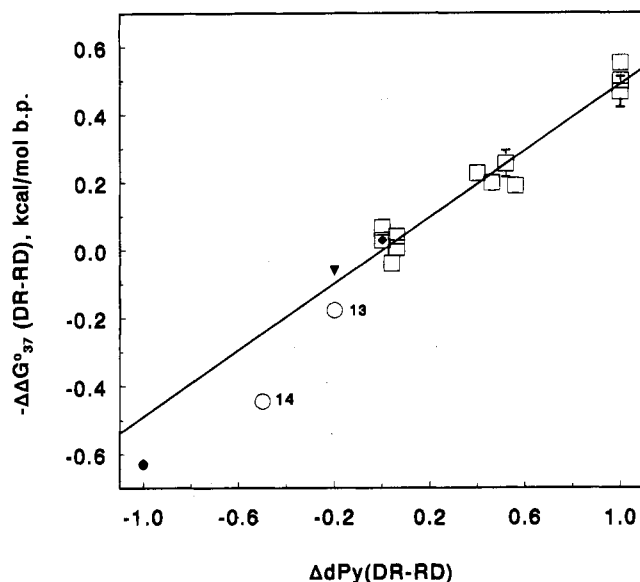


FIGURE 3: Effect of deoxypyrimidine fraction in hybrid on relative hybrid stability of hybrid pairs: Relationship between the difference in free energy of duplex formation for matched pairs of DR and RD hybrids and the difference in dPy fraction in their DNA strands. Shown are  $\Delta\Delta G^\circ_{37}$  values for groups A, B, and C ( $\square$ ) and group D ( $\circ$ ). Solid lines are linear fits of the data for groups A, B, and C. Also shown are data from Hall and McLaughlin (1991) ( $\blacktriangledown$ ) and Ratmeyer et al. (1994) ( $\blacklozenge$ ).

also increased with an increase of deoxypyrimidine fraction. Hybrids with DNA strands containing less than 30% deoxypyrimidines were less stable than the DNAs. Hybrids with DNA strands containing 70–100% deoxypyrimidines were more stable than the DNAs.  $\Delta T_M(\text{DD-hybrid})$  values were  $-14 \pm 2^\circ\text{C}$  for hybrids with 100% dPy in the DNA strand. (The plot for  $\Delta T_M(\text{DD-hybrid})$  vs dPy content is included in supporting information.) A deoxypyrimidine content of about 50% is the “break-even” point. Large variations in ratios of  $\Delta G^\circ_{37}$  observed in Figure 4 indicate that additional factors also affect relative hybrid stability.

**CD Spectra of Hybrids of Groups A–C.** Eight sequences out of 14 (seqs 2 and 3 from group A, seqs 5 and 6 from group B, seqs 9 and 12 from group C, and seqs 13 and 14 from group D) were chosen for studies of hybrid geometry. In Figure 5, we plot CD spectra for five sequences. For each sequence, four duplexes (RR, DD, DR, RD) were evaluated. Figure 5 indicates that all hybrids generated CD spectra intermediate between DNA and RNA spectra, though they differed noticeably in details.

For groups A and B, spectra of DR ( $\geq 70\%$  dPy) hybrids are different from those of RD ( $\leq 30\%$  dPy) hybrids (Figure 5a,b). Intensities of the major positive bands in the DR spectra were close to the intensity of the corresponding DNA bands, whereas the intensities of the negative bands at 210 nm were very close to those of the corresponding RNA bands. RD hybrids generated spectra with a major positive band which was more intense than the corresponding RNA band and with a negative band at 210 nm with an intensity similar to the intensity of the corresponding DNA band. These spectra were very similar to reported spectra of homopurine–homopyrimidine hybrid duplexes (Roberts & Crothers, 1992; Ratmeyer et al., 1994; Hung et al., 1994).

DR and RD hybrid pairs from group C with 50% deoxypyrimidine in both strands generated spectra with an intensity at 210 nm between those of the corresponding DNA

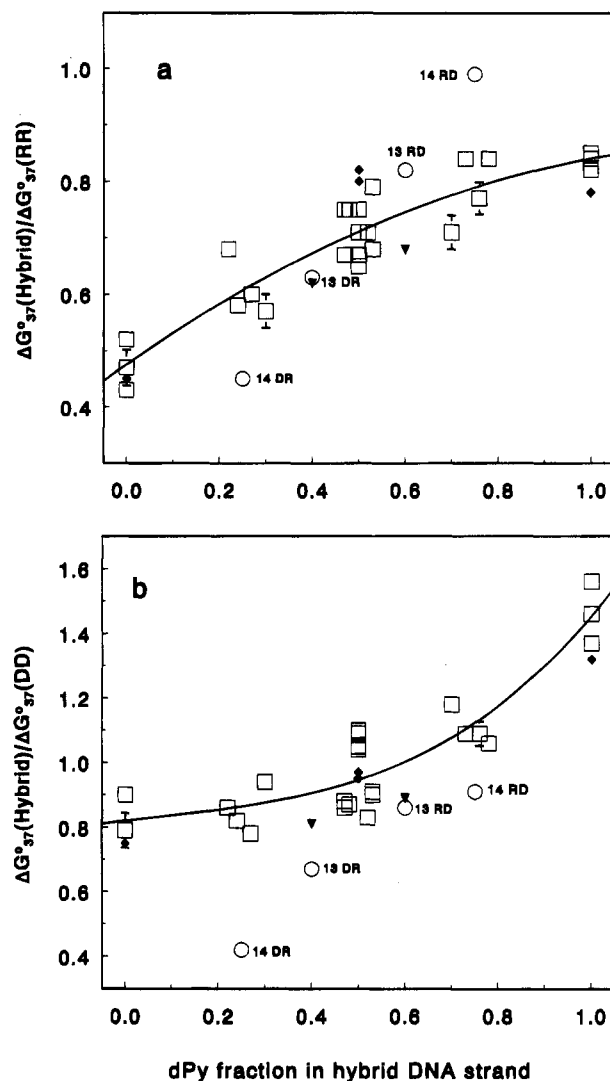


FIGURE 4: Effect of deoxypyrimidine fraction in hybrid on relative hybrid stability compared to RNA and DNA counterparts: Ratios of free energies of hybrids to RNA (a) and DNA (b) counterparts. Shown are  $\Delta G^\circ_{37}$  values for groups A, B, and C ( $\square$ ) and for group D ( $\circ$ ). Solid lines are drawn through the data for groups A, B, and C. Also shown are data from (Ratmeyer et al. (1994) ( $\blacklozenge$ ) and Hall and McLaughlin (1991) ( $\blacktriangledown$ ).

and RNA bands (Figure 5c,d). Intensities and positions of the major positive bands were different for the two sequences. The hybrids with a low A·T/U fraction had major positive bands with intensities close to that of the corresponding RNA band (Figure 5c, seq 9). Hybrids with moderate and high A·T/U fractions generated spectra with the major positive bands similar to the average of the corresponding RNA and DNA bands (Figure 5d, seq 12).

Observations indicated that relative intensities of hybrid bands at 210 nm correlated well with dPy content in hybrids (Figure 6a). A higher deoxypyrimidine content resulted in a more RNA-like CD band at 210 nm. This trend was also observed by Ratmeyer et al. (1994) and Hung et al. (1995) for repeating sequences.

**Electrophoretic Mobility of Hybrids on Native Polyacrylamide Gels.** We also used PAGE to investigate the conformational properties of hybrid duplexes. Four duplexes, RR, DR, RD, and DD, of nine sequences from groups A–D (Table 1, seqs 1–3, 5, 6, 9, and 12–14) were run on native 20% polyacrylamide gels in TBM buffer. As observed by

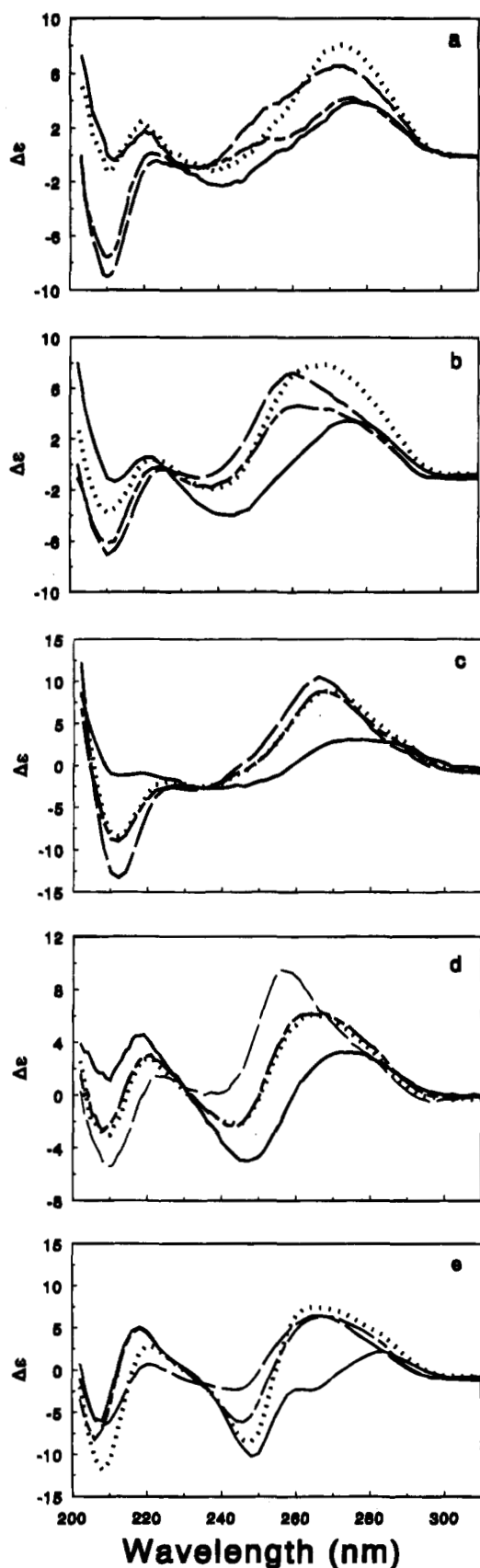


FIGURE 5: Circular dichroism spectra of RR (---), DD (—), DR (— — —), and RD (····) duplexes of seqs 3 (a), 6 (b), 9 (c), 12 (d), and 14 (e). (For experimental conditions, see Materials and Methods; sequences are presented in Table 1.)

others (Bhattacharyya et al., 1990; Roberts & Crothers, 1992; Ratmeyer et al., 1994), RNA duplexes always migrated

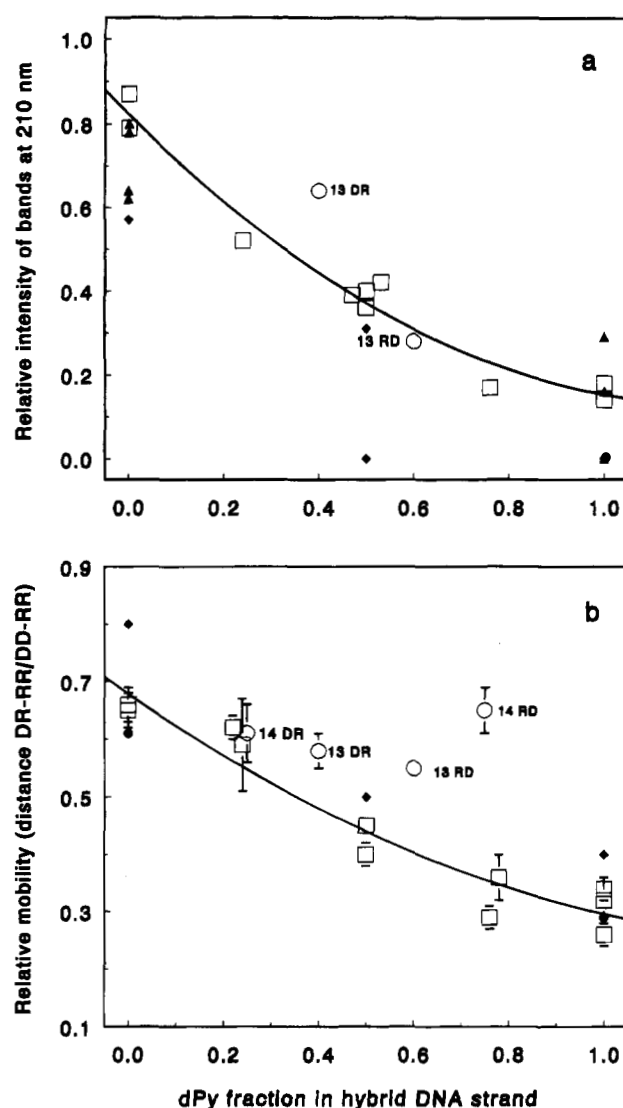


FIGURE 6: Effect of deoxypyrimidine fraction in hybrid on relative intensity of CD bands at 210 nm [ $\Delta\epsilon_{210}(\text{RR}) - \Delta\epsilon_{210}(\text{hybrid})$ ]/ $[(\Delta\epsilon_{210}(\text{RR}) - \Delta\epsilon_{210}(\text{DD}))]$  (a) and relative hybrid mobility on native 20% polyacrylamide gel [distance(hybrid-RR)/distance(DD-RR)] (b) for hybrid duplexes of groups A, B, and C ( $\square$ ) and group D ( $\circ$ ). Solid lines are drawn through the data for groups A, B, and C. [CD data for seq 14 are not shown because of the anomalous intensities of the RNA and DNA bands at 210 nm (see text). Relative mobility of the RD hybrid of seq 3 is not shown because the hybrid melted during electrophoresis.] Also shown are data from (Hung et al. (1995) ( $\blacktriangle$ ), Ratmeyer et al. (1994) ( $\blacklozenge$ ), and Roberts and Crothers (1992) ( $\bullet$ )).

slower than corresponding DNA duplexes. The mobility of both species depended on duplex length and demonstrated a linear correlation with reciprocal number of base pairs or molecular masses (see supporting information). The electrophoretic behavior of hybrids depended both on duplex length and on the base composition of the DNA strand. Relative hybrid mobility calculated as the ratio of the distance between RNA and hybrid species to the distance between RNA and DNA species for each sequence correlated with pyrimidine content in the hybrid DNA strand (Figure 6b). Hybrids with high dPy content ran nearer to RNA, and hybrids with low dPy ran nearer to DNA. Relative mobilities calculated from data presented by Roberts and Crothers (1992) and Ratmeyer et al. (1994) are reasonably consistent with the results obtained in our experiment (Figure 6b).

**Group D with (A)<sub>n</sub> Strings.** The thermodynamic properties of both RNA and DNA counterparts and hybrid duplexes with (A)<sub>n</sub> strings (group D, seqs 13 and 14) did not obey the correlations found for other sequences with mixed purine–pyrimidine base composition and similar GC content (Figures 1–4). For seq 13 with an (A)<sub>5</sub> string making up only 33% of the 15-mer sequence, the deviations were not as great as for seq 14 with an (A)<sub>10</sub> string making up 62% of 16-mer sequence.

First, the DNA duplexes of seqs 13 and 14 displayed enhanced stability compared to the stability predicted for mixed DNAs. On the other hand, the stabilities of the RNA and DR hybrid of seq 14 were substantially lower than the stabilities of other duplexes with similar base composition (Figures 1 and 2). As a result,  $\Delta\Delta G^{\circ}_{37}(\text{DR-RD})$  for hybrids of seq 14 fell far from the line in Figure 3. Also the  $\Delta G^{\circ}_{37}(\text{hybrid})/\Delta G^{\circ}_{37}(\text{RR})$  ratio for the RD hybrid of seq 14 was very high due to the reduced stability of RNA (Figure 4a) and the  $\Delta G^{\circ}_{37}(\text{hybrid})/\Delta G^{\circ}_{37}(\text{DD})$  ratio for hybrid DR of seq 14 was too low due to the enhanced stability of DNA and the reduced stability of the DR duplex (Figure 4b).

CD spectra of duplexes of seq 14 also differed from those for other duplexes studied in these experiments (Figure 5e). Both the DR and RD hybrids of seq 14 generated CD spectra with positive bands at 270 nm which were similar to the RNA band, with negative bands at 250 nm which were close to the DNA band or intermediate between those for RNA and DNA duplexes, and with negative bands at 210 nm which were more intense (especially in the RD spectrum) than the corresponding band in the RNA spectrum. It should be noted that the DNA duplex of seq 14 also generated an unusual spectrum with a negative band at 210 nm of the same intensity as the RNA duplex. PAGE experiments also suggested some peculiarities in the mobility of hybrids of seqs 13 and 14. RD hybrids of seq 13 and especially of seq 14 with (rA)<sub>n</sub>(dT)<sub>n</sub> strings migrated anomalously fast (Figure 6b).

## DISCUSSION

The successful utilization of antisense deoxyoligonucleotides as therapeutics requires good hybridization of oligonucleotides to cellular RNA and DNA targets. Although thermodynamic parameters are available for predicting stability of RNA and DNA duplexes in 1 M NaCl (Freier et al., 1986; Breslauer et al., 1986), no rules for prediction of hybrid stability especially for relatively long oligonucleotides ( $12 < N < 22$ ) under physiological conditions are available. Our goal was to evaluate the effect of base composition on stability and conformation of hybrid duplexes and compare them to the stability and conformation of their RNA and DNA counterparts in solution at moderate Na<sup>+</sup> concentration.

Duplex free energies were derived from fitting melting curves using a modified two-state model (Petersheim & Turner, 1983) which is most appropriate for duplexes shorter than 12 base pairs (Breslauer et al., 1975). Therefore, it was important to evaluate whether the stability of long oligonucleotide duplexes obeys the same correlations as those of short duplexes. In our study six of 14 sequences were equal to or shorter than 12 bases long. Seven were between 15 and 18 bases long, and one oligonucleotide was 21 bases long. In each group except group D there were oligomer sequences with lengths shorter and longer than 12 bases.

Reported correlations of relative hybrid stability with base composition were observed for both short ( $N \leq 12$ ) and long ( $N \geq 15$ ) duplexes, suggesting that our duplex stabilities may be valid. Free energies of duplex formation obtained from absorbance vs temperature curves are sensitive to the method of analysis (Albergo et al., 1981; Petersheim & Turner, 1983; Nelson et al., 1981) and depend critically on the two-state nature of the transition. In contrast,  $T_M$  values are insensitive to the method of analysis and do not depend on the two-state nature of the transition (Albergo et al., 1981; Petersheim & Turner, 1983; Nelson et al., 1981). Our analyses (e.g., Figures 3 and 4) were performed using both  $\Delta G^{\circ}_{37}$  ratios (or  $\Delta\Delta G^{\circ}_{37}$ ) and  $\Delta T_M$  values (see supporting information). Trends were similar for both plots, suggesting that deviations from two-state behavior would not affect the correlations. In addition, thermodynamic parameters obtained by Hall and McLaughlin (1991) and Ratmayer et al. (1994) for short duplexes from oligonucleotide concentration dependencies under conditions favorable for true two-state transitions fall close to our curves in Figures 3 and 4, providing further support for our use of a two-state model to analyze our data.

**Stability of Hybrids Relative to Their RNA and DNA Counterparts.** Data presented in Figure 4a,b indicates that  $\Delta G^{\circ}_{37}(\text{hybrid})/\Delta G^{\circ}_{37}(\text{RR})$  and  $\Delta G^{\circ}_{37}(\text{hybrid})/\Delta G^{\circ}_{37}(\text{DD})$  ratios for hybrids with similar dPy content vary significantly, suggesting dPy content is only one of the factors affecting relative hybrid stability. In Figure 7 we plotted  $\Delta\Delta G^{\circ}_{37}(\text{hybrid-RR})$  and  $\Delta\Delta G^{\circ}_{37}(\text{hybrid-DD})$  values vs A•T/U base pair content for hybrids with different dPy fractions in DNA strands. The plots in Figure 7 clearly demonstrate that the stability of hybrids relative to RNA or DNA duplexes depends weakly on the amount of A•T/U base pairs over the range of 40–80% of total base pairs. However, when the A•T/U fraction became less than 30–35% of total length, the relative stability of hybrids decreased dramatically compared to RNA counterparts and increased compared to DNAs. Analysis of the data (see supporting information) shows that the decrease of A•T/U base pair content from 80 to 40–35% of total base pairs results in a similar increase of RR, DD, and hybrid stability. However, when A•T/U base pair content drops lower than 35%, the stability of the RNAs increases sharply, whereas the stability of the DNAs keeps increasing gradually. Hybrid stability also increases significantly but to a lesser extent than the stability of RNA duplexes. As result, hybrids of seqs 4, 8, and 9 with low A•T/U base pair content, in contrast to other hybrids in groups B and C, were more stable than their DNA counterparts but less stable than their RNA counterparts (Figure 7).

Thus, the deviations from the curves in Figure 4 reflect the different relative stability of hybrids with the same dPy fraction and a different A•T/U content. Analysis of  $T_M$  data reported by Hung et al. (1995) for homopurine–homopyrimidine hybrids indicates that the variation in  $\Delta T_M(\text{RR-hybrid})$  values correlates with A•T/U content in the same way. A substantial increase of hybrid stability at low A•T/U content may be due to the enhanced ability of G+C-rich DNA strands to adopt an A-like conformation. This is consistent with observations that the facility of the B → A transitions increases with increased total (G+C) content in DNA duplexes (Pilet & Brahms, 1972; Minchenkova et al., 1986; Becker & Wang, 1989).

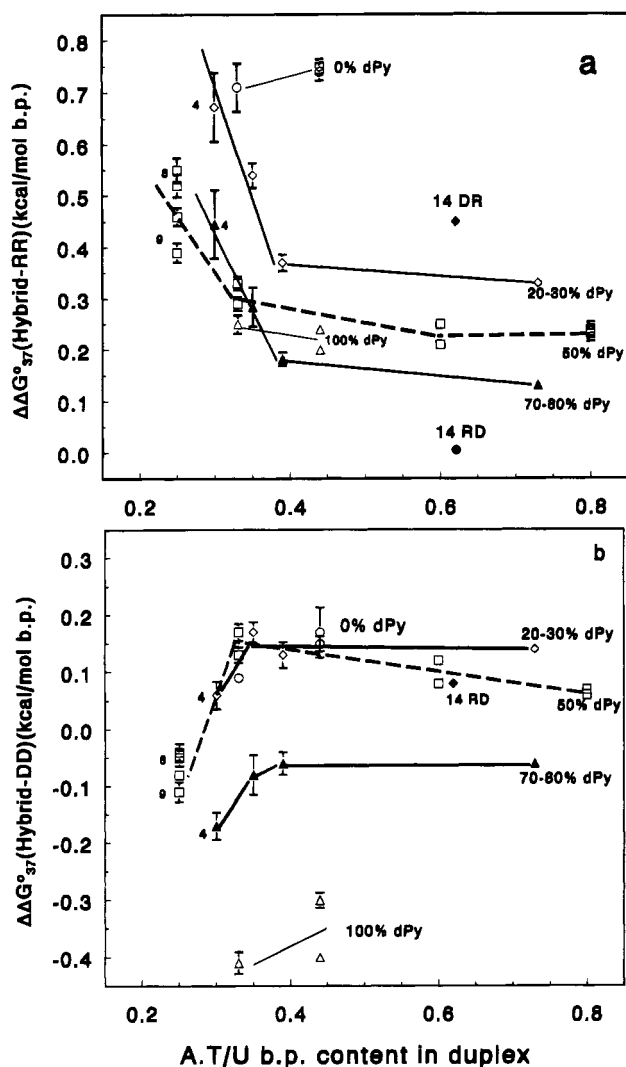


FIGURE 7: Effect of A:T/U content on the difference in free energies of hybrid and RNA duplex formation (a) or hybrid and DNA duplex formation (b) for hybrids of groups A, B, and C with 0% (○), 22–30% (◇), 47–53% (□), 70–78% (△), and 100% (▽) dPy content in DNA strand.

**Relationship between Thermodynamic Stability and Hybrid Conformation Based on CD and PAGE Data.** Both CD and PAGE data provide evidence of the relationship between hybrid conformation and stability. Analysis of CD spectra of 16 hybrids (spectra for 10 of them are presented in Figure 5) indicated that the intensity and position of the major positive band near 270 nm in the hybrid spectrum depended primarily on the overall GC content of duplexes. The relative intensity of the negative band at 210 nm for all hybrids studied was slightly affected by base composition and correlated qualitatively with deoxypyrimidine content in the hybrid (Figure 6). Hung et al. (1995) demonstrated that the formation of A-form oligoribonucleotide duplexes from single strands results in a substantial increase of the intensity of the negative band at 210 nm, whereas the intensity of the band at 260–270 nm is close to the sum of the intensities of the corresponding bands in the single-strand spectra, suggesting that the 210-nm band is more sensitive to A-form oligoduplex formation than the band at 260 nm. Assuming that the closer hybrid conformation is to A-form, the closer the intensity of the hybrid 210-nm band is to the intensity of the corresponding RNA band, we evaluated the conformation of the hybrid helix using the ratio  $[\Delta\epsilon_{210}(\text{RR}) - \Delta\epsilon_{210}(\text{Hybrid})]/[\Delta\epsilon_{210}(\text{RR}) - \Delta\epsilon_{210}(\text{DD})]$ . Because the relative intensity of the 210-nm band and the ratio of  $\Delta\Delta G_{37}^{\circ}$  values for the hybrid and RNA duplexes both correlate with the dPy fraction in the hybrid (Figures 4a and 6a), there is a correlation between these two parameters (Figure 8a). The plot in Figure 8a indicates that more stable hybrids generate CD spectra with 210-nm bands whose intensities are closer to the corresponding RNA bands than less stable hybrids do. The smooth correlation curve suggests there is a continuum of intermediate hybrid conformers between A- and B-form. These data are easy to interpret within the framework of the model suggesting that deoxyriboses in hybrid duplex undergo rapid exchange mainly between S and N conformations (Gonzalez et al., 1994, 1995). On the basis of this model, we can suggest that increasing the dPy fraction in the hybrid results in a shift of the  $S \leftrightarrow N$  equilibrium toward the N domain and the formation of more stable duplex.

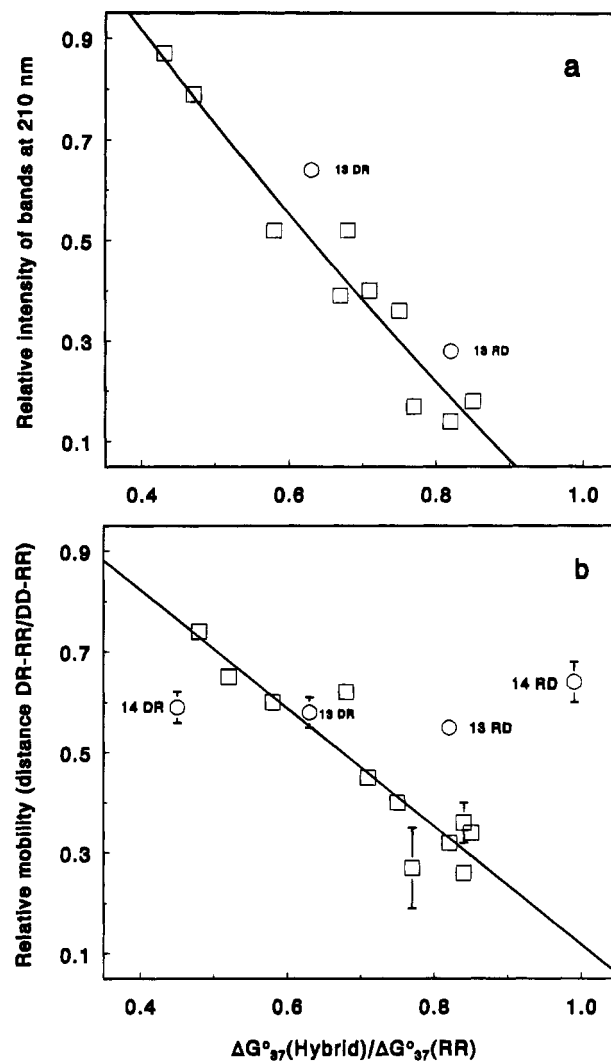


FIGURE 8: Relationships between relative stabilities and relative intensities of bands at 210 nm in hybrid CD spectra (a) and relative mobilities of hybrids on native 20% polyacrylamide gel in TBM buffer (b): Relative intensities of bands at 210 nm in CD spectra and relative mobilities of hybrids of groups A, B, and C (□) and group D (○). Numbers near the markers designate the numbers of sequences in Table 1.

Because the relative intensity of the 210-nm band and the ratio of  $\Delta\Delta G_{37}^{\circ}$  values for the hybrid and RNA duplexes both correlate with the dPy fraction in the hybrid (Figures 4a and 6a), there is a correlation between these two parameters (Figure 8a). The plot in Figure 8a indicates that more stable hybrids generate CD spectra with 210-nm bands whose intensities are closer to the corresponding RNA bands than less stable hybrids do. The smooth correlation curve suggests there is a continuum of intermediate hybrid conformers between A- and B-form. These data are easy to interpret within the framework of the model suggesting that deoxyriboses in hybrid duplex undergo rapid exchange mainly between S and N conformations (Gonzalez et al., 1994, 1995). On the basis of this model, we can suggest that increasing the dPy fraction in the hybrid results in a shift of the  $S \leftrightarrow N$  equilibrium toward the N domain and the formation of more stable duplex.

Relative mobilities of hybrids provide additional characteristics of hybrid helix conformation. PAGE data demonstrate that hybrids migrate differently relative to their RNA

and DNA counterparts depending on deoxypyrimidine content (Figure 6b). Slow migration of short RNA duplexes compared to DNA on small-pore gels apparently reflects the difference in the overall size, shape, and flexibility of A- and B-helices (Roberts & Crothers, 1992). If it is so, the difference in hybrid mobility on 20% polyacrylamide gel also likely reflects the difference in their geometry and conformational properties. Smooth variation of hybrid relative mobility with dPy content suggests the existence of a wide continuum of intermediate hybrid conformations. Correlation between relative mobility and relative hybrid stability (Figure 8b) supports the suggestion of a relationship between helix conformation and thermodynamic stability of hybrid duplexes.

**Structural Peculiarities and Thermodynamic Stability of Duplexes with  $(A)_n(T/U)_n$  Tracts.** The deviations in relative hybrid stability of seqs 13 and 14 may be related to the conformational peculiarities of both hybrids and their RNA and DNA counterparts. It has been postulated (Dickerson et al., 1982; Kopka et al., 1983) that a hydration water spine in the minor groove of  $(dA)_n(dT)_n$  sequences is greatly responsible for the unusual B'-conformation and enhanced stability of duplex. Our data on seq 13 and especially on seq 14 confirm the stabilization effect of  $(dA)_5(dT)_5$  and  $(dA)_{10}(dT)_{10}$  tracts in DNA duplexes. The water spine in the minor groove of  $(dA)_n(dT)_n$  sequences in DNA duplexes is supposed to impede the B  $\rightarrow$  A transition under dehydrated conditions (Dickerson et al., 1982). There is no data about hydration of  $(dA)_n(rU)_n$  sequences. However, the very low stability of hybrids with long  $(dA)_n(rU)_n$  tracts reported by Martin and Tinoco (1980) and demonstrated in our experiments allows us to speculate that the S  $\rightarrow$  N conformational shift of  $(dA)_n$  tracts which may be necessary to produce a stable hybrid helix is also impeded by enhanced hydration of  $(dA)_n(rU)_n$  tracts in a narrowed (relative to A-form) minor groove (Arnott et al., 1986; Fedoroff et al., 1993; Gonzalez et al., 1995). Some peculiarities in RR, DD, and hybrid structures are supported by CD and PAGE data. In contrast to all other sequences examined, the CD intensities at 210 nm for RR and DD duplexes for seq 14 were similar (Figure 5e). For the RD hybrid with an  $(rA)_{10}(dT)_{10}$  tract, the CD at 210 nm is twice as intense as that generated by the RR duplex, suggesting that the structure of the RD hybrid is close to A-form. However, the electrophoretic mobility of the RD hybrid was close to the mobility of hybrids with low deoxypyrimidine content whose conformations are supposed to be far from A-form (Figure 6b). The enhanced mobility of the hybrid with a  $(rA)_{10}(dT)_{10}$  tract may result from an unusual compact hybrid structure caused by hydrophobic interactions between the 5-methyl groups of 10 consecutive thymines.

**Relative Stability of Hybrid Duplexes and Antisense Activity of Oligonucleotides.** Antisense oligonucleotides were designed to bind viral and neoplastic mRNAs and inhibit gene expression. Any mechanism of antisense inhibition in cells requires hybridization of DNA oligonucleotides to an mRNA target which possesses its own secondary and tertiary structure. Frequently antisense oligonucleotides are assumed to bind both loop and stem parts of mRNA hairpins (Monia et al., 1993; Bennett & Crooke, 1994). Therefore, hybrid duplex formation requires opening of the mRNA stem for hybridization of the DNA oligonucleotide to the complementary RNA region. In this competitive

situation, relative stability of a hybrid compared to the RNA duplex becomes more important than an absolute hybrid stability. The most stable hybrids form if homopyrimidine DNAs bind homopurine RNA targets (Figure 2); however, homopurine-homopyrimidine RNA duplexes are also extraordinarily stable (Figure 1). As a result, the relative stability of homopurine-homopyrimidine hybrids does not exceed the relative stability of hybrids containing 70–80% deoxypyrimidines (Figure 7a).  $\Delta\Delta G^\circ_{37}(\text{hybrid-RR})$  values calculated from data reported by Ratmeyer et al. (1994) also indicate that the relative stability of hybrids with 100% dPy is lower than that of hybrids with 50% dPy. Using  $\Delta\Delta G^\circ_{37}(\text{hybrid-RR})$  values, we can calculate the ratio of the equilibrium constants for RNA and hybrid duplex formation. Therefore, smaller  $\Delta\Delta G^\circ_{37}$  values correspond to stronger competitive binding to structured RNA. Thus, one can suggest that, under otherwise equal conditions, antisense oligonucleotides with 70–80% deoxypyrimidine content and moderate A•T/U content will be most effective at targeting structured mRNA.

To test this hypothesis, we examined whether a correlation between dPy and (A+T) base content with biological activity existed for 33 oligonucleotides targeted to different regions of human E-selectin and VCAM-1 genes (Bennett et al., 1994). (Sequences and activities of these oligonucleotides are included in the supporting information.) Among the six most effective oligomers, five had 70–80% and one had 60% deoxypyrimidines and all of them had 40–50% (A+T) content. However, two sequences with 75 and 86% deoxypyrimidines demonstrated low antisense activity. These data indicate that there is no simple correlation between antisense activity and hybridization properties of DNA oligonucleotides to single-stranded RNA targets in solution because many other factors affect activity of antisense oligonucleotides (Lima et al., 1992). However, the likelihood is higher that oligonucleotides with 70–80% pyrimidine fraction and moderate (A+T) content will be more successful in antisense binding than oligonucleotides with low deoxypyrimidine fraction or very low (A+T) base content.

## ACKNOWLEDGMENT

We thank Dr. Ignacio Tinoco Jr. of the University of California at Berkeley for the use of his circular dichroism spectrophotometer, Dr. Maryann Zounes and Pierre Villiet for synthesis and purification of DNA and RNA oligonucleotides, Drs. David J. Ecker and Ignacio Tinoco Jr. for helpful discussions, and Mrs. Carol Collins for excellent secretarial help.

## SUPPORTING INFORMATION AVAILABLE

Figures providing plots of  $\Delta T_M(\text{DR-RD})$  vs  $\Delta d\text{Py}(\text{DR-RD})$  for hybrids (analog of Figure 3);  $\Delta T_M(\text{RR-hybrid})$  and  $\Delta T_M(\text{DD-hybrid})$  vs  $\Delta d\text{Py}$  fraction in hybrids (analog of Figure 4); relative mobility of DNA and RNA species vs length of duplexes;  $\Delta G^\circ_{37}$  values for RR, DD, DR, and RD duplexes of groups B and C vs A•T/U bp content, and two tables from Bennett et al. (1994) listing sequences, biological activities, and added dPy and (A+T) content for antisense oligonucleotides targeting human E-selectin and VCAM-1 genes (5 pages). Ordering information is given on any current masthead page.

## REFERENCES

- Albergo, D. D., Marky, L. A., Breslauer, K. J., & Turner, D. H. (1981) *Biochemistry* 20, 1409.
- Arnott, S., Chandrasekaran, R., Millane, R. P., & Park, H.-S. (1986) *J. Mol. Biol.* 188, 631.
- Becker, M. M., & Wang, Z. (1989) *J. Biol. Chem.* 264, 4163.
- Benevides, J. M., & Thomas, G. J., Jr. (1988) *Biochemistry* 27, 3868.
- Bennett, C. F., & Crooke, S. T. (1994) *Adv. Pharmacol.* 28, 1.
- Bennett, C. F., Condon, T., Grimm, S., Chan, H., & Chiang, M.-Y. (1994) *J. Immunol.* 152, 3530.
- Bhattacharyya, A., Murchie, A. I. H., & Lilley, D. M. (1990) *Nature* 343, 484.
- Breslauer, K. J., Sturtevant, J. M., & Tinoco, I., Jr. (1975) *J. Mol. Biol.* 99, 549.
- Breslauer, K. J., Frank, R., Blocker, H., & Marky, L. A. (1986) *Proc. Natl. Acad. Sci. U.S.A.* 83, 3746.
- Chamberlin, M., & Patterson, D. (1965) *J. Mol. Biol.* 12, 410.
- Chou, S.-H., Flynn, P., & Reid, B. (1989) *Biochemistry* 28, 2435.
- Crooke, S. T. (1992) *Annu. Rev. Pharmacol. Toxicol.* 32, 329.
- Dickerson, R. E., Drew, H. R., Conner, B. N., Wing, R. M., Fratini, A. V., & Kopka, M. L. (1982) *Science* 216, 475.
- Fedoroff, O. Y., Salazar, M., & Reid, B. R. (1993) *J. Mol. Biol.* 233, 509.
- Freier, S. M., Kierzek, R., Jaeger, J. A., Sugimoto, N., Caruthers, M. H., Neilson, T., & Turner, D. H. (1986) *Proc. Natl. Acad. Sci. U.S.A.* 83, 9373.
- Fujiwara, T., & Shindo, H. (1985) *Biochemistry* 24, 896.
- Gonzalez, C., Stec, W., Kobylanska, A., Hogrefe, R. I., Reynolds, M., & James, T. L. (1994) *Biochemistry* 33, 11062.
- Gonzalez, C., Stec, W., Reynolds, M., & James, T. L. (1995) *Biochemistry* 34, 4969.
- Gray, D. M., & Ratliff, R. L. (1975) *Biopolymers* 14, 487.
- Hall, K. B., & McLaughlin, L. W. (1991) *Biochemistry* 30, 10606.
- Hung, S.-H., Yu, Q., Gray, D. M., & Ratliff, R. L. (1994) *Nucleic Acids Res.* 22, 4326.
- Katahira, M., Lee, S. J., Kobayashi, Y., Sugeta, H., Kyogoku, Y., Iwai, S., Ohtsuka, E., Benevides, J. M., & Thomas, G. J., Jr. (1990) *J. Am. Chem. Soc.* 112, 4508.
- Kirkpatrick, D. P., & Radding, C. M. (1992) *Nucleic Acids Res.* 20, 4347.
- Kopka, M. L., Fratini, A. V., Drew, H. R., & Dickerson, R. E. (1983) *J. Mol. Biol.* 163, 129.
- Lesnik, E. A., Guinasso, C. J., Kawasaki, A. M., Sasmor, H., Zounes, M., Cummins, L. L., Ecker, D. J., Cook, P. D., & Freier, S. M. (1993) *Biochemistry* 32, 7832.
- Lima, W. F., Monia, B. P., Ecker, D. J., & Freier, S. M. (1992) *Biochemistry* 31, 12055.
- Martin, F. H., & Tinoco, I. J. (1980) *Nucleic Acids Res.* 8, 2295.
- Minchenkova, L. E., Schyolkina, A. K., Chernov, B. K., & Ivanov, V. I. (1986) *J. Biomol. Struct. Dyn.* 4, 463.
- Monia, B. P., Johnston, J. F., Ecker, D. J., Zounes, M., Lima, W. F., & Freier, S. M. (1992) *J. Biol. Chem.* 267, 19954.
- Monia, B. P., Lesnik, E. A., Gonzalez, C., Lima, W. F., McGee, D., Guinasso, C. J., Kawasaki, A. M., Cook, P. D., & Freier, S. M. (1993) *J. Biol. Chem.* 268, 14514.
- Nelson, J. W., Martin, F. H., & Tinoco, I. J. (1981) *Biopolymers* 20, 2509.
- O'Brien, E. J., & MacEvan, A. W. (1970) *J. Mol. Biol.* 48, 243.
- Ogawa, T., & Okazaki, T. (1980) *Annu. Rev. Biochem.* 49, 421.
- Pardi, A., Martin, F. H., & Tinoco, I. J. (1981) *Biochemistry* 20, 3986.
- Petersheim, M., & Turner, D. H. (1983) *Biochemistry* 22, 256.
- Pilet, J., & Brahms, J. (1972) *Nature* 236, 99.
- Ratmeyer, L., Vinayak, R., Zhong, Y. Y., Zon, G., & Wilson, W. D. (1994) *Biochemistry* 33, 5298.
- Riley, M., Maling, B., & Chamberlin, M. J. (1966) *J. Mol. Biol.* 20, 359.
- Roberts, R. W., & Crothers, D. M. (1992) *Science* 258, 1463.
- Salazar, M., Fedoroff, O. Y., Miller, J. M., Ribeiro, N. S., & Reid, B. R. (1993) *Biochemistry* 32, 4207.
- Shindo, H., & Matsumoto, U. (1984) *J. Biol. Chem.* 259, 8682.
- Varmus, H. E. (1982) *Science* 216, 812.

BI9504623